Supplementary Information (SI) for CrystEngComm.
This journal is © The Royal Society of Chemistry 2024

Supporting information to:

Impurity-induced Acceleration of Polymorphic Conversion via Crystalline Solid Solutions and the T-X Phase Diagrams of Salicylic acid and 3-Hydroxybenzoic acid

Tao Zhang, Francesco Ricci, Seyed Sepehr Mohajerani, Mitchell Paolello, Fredrik L. Nordstrom*

Material & Analytical Sciences, Boehringer-Ingelheim, Ridgefield, 06877, Connecticut, USA. Email: fredrik.nordstrom@boehringer-ingelheim.com

Department of Physics, Stevens Institute of Technology, Hoboken, 07030, New Jersey, USA

Department of Chemical Engineering, Rowan University, Glassboro, 08028, New Jersey, USA

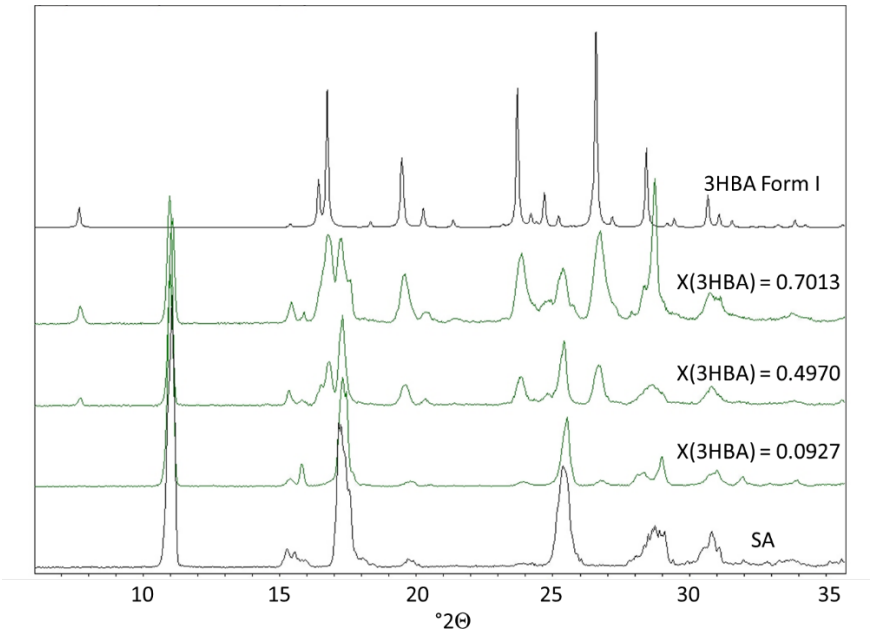

Figure 1. XRPD overlay of select SA-3HBA Form I samples used in DSC analyses.

Table 1. DSC summary for SA-3HBA Form I

X(3HBA)	DSC endotherms	Low temperature endotherm					High temperature endotherm				
mol 3HBA/mol SA+3HBA		T_{inset}	T_{onset}	T_{peak}	T_{offset}	Enthalpy	T_{inset}	T_{onset}	T_{peak}	T_{offset}	Enthalpy
		°C	°C	°C	°C	J/g	°C	°C	°C	°C	J/g
0	One endotherm						154.07 (0.08)	158.64 (0.006)	159.16 (0.09)	160.98 (0.23)	189.56 (4.21)
0.0031	One endotherm						152.33 (0.26)	158.41 (0.32)	158.83 (0.10)	160.86 (0.64)	178.97 (13.18)
0.0050	One endotherm						151.87 (0.57)	157.55 (0.20)	158.70 (0.09)	160.33 (0.23)	174.50 (3.49)
0.0099	Two partially overlapping endotherms	143.14 (0.56)	145.01 (1.08)	147.39 (0.16)	149.33[1] (0.66)	7.59 (4.45)		157.11 (0.80)	158.74 (0.20)	160.53 (0.02)	168.97 (10.7)
0.0177	Two partially overlapping endotherms	141.12 (0.45)	145.70 (1.11)	147.13 (0.42)	149.72[1] (1.52)	14.19 (6.53)		155.95 (0.88)	158.35 (0.28)	160.44 (0.39)	168.84 (8.47)
0.0443	Two partially overlapping endotherms	140.27 (0.14)	144.06 (0.20)	147.47 (0.22)	149.72[1] (1.12)	42.22 (10.97)		153.98 (0.95)	157.33 (0.90)	159.48 (0.50)	132.71 (20.71)
0.0927	Two partially overlapping endotherms	140.10 (0.10)	143.97 (0.03)	147.23 (0.09)	149.81[1] (0.09)	88.25 (1.55)			155.03 (0.32)	157.50 (0.22)	91.92 (5.15)
0.1463	Two endotherms mostly overlapping	140.50 (0.11)	144.33 (0.03)	146.50 (0.22)	149.40[1] (0.16)	138.06 (9.42)			152.50 (0.26)	155.27 (0.95)	54.78 (9.03)
0.1984	Two endotherms mostly overlapping	140.35 (0.29)	144.44 (0.03)	146.68 (0.39)	149.36[1] (0.05)	156.82 (14.87)				154.48 (0.73)	38.24 (12.97)
0.2378	Two endotherms mostly overlapping	141.02 (0.32)	144.49 (0.02)	146.84 (0.32)	148.81[1] (0.22)	188.32 (8.12)				154.97 (1.49)	5.74 (5.44)
0.2993	Two endotherms mostly overlapping	140.65 (0.01)	144.64 (0.06)	146.46 (0.37)	149.70[1] (0.14)	183.99 (5.05)				160.13 (1.78)	11.77 (6.26)
0.3947	Two endotherms mostly overlapping	140.47 (0.26)	144.72 (0.07)	146.42 (0.09)	149.62[1] (0.16)	171.99 (6.19)				167.81 (3.80)	26.13 (7.14)
0.4970	Two partially overlapping endotherms	139.61 (0.30)	144.66 (0.01)	146.05 (0.07)	149.58[1] (0.53)	135.75 (10.27)			171.72 (2.24)	179.64 (3.10)	71.79 (16.00)
0.6005	Two partially overlapping endotherms	139.73 (0.01)	144.80 (0.01)	146.38 (0.28)	149.35[1] (0.11)	117.25 (4.10)			180.13 (7.58)	188.24 (6.06)	99.63 (11.92)

0.7013	Two partially overlapping endotherms	139.77 (0.96)	144.25 (0.11)	146.19 (0.14)	148.51[1] (0.25)	70.88 (7.34)		183.38 (5.55)	189.24 (2.59)	193.74 (2.41)	158.78 (39.29)
0.8073	Two mostly separated endotherms	138.16 (1.52)	145.67 (2.12)	146.57 (0.20)	149.44[1] (0.58)	37.83 (6.59)		201.44 (0.03)	200.22 (3.42)	202.57 (2.59)	198.76 (4.61)
0.8987	Two mostly separated endotherms	138.54 (0.79)	141.79 (2.27)	145.86 (0.97)	148.65[1] (0.87)	7.74 (4.05)		201.35 (0.07)	202.07 (0.11)	204.25 (0.26)	238.56 (2.63)
0.9504	One endotherm						183.73 (0.25)	201.51 (0.27)	202.15 (0.25)	204.78 (0.37)	246.14 (3.24)
0.9601	One endotherm						186.84 (1.38)	201.38 (0.11)	202.25 (0.15)	204.64 (0.23)	244.64 (13.22)
0.9702	One endotherm						187.60 (0.70)	201.36 (0.14)	202.14 (0.14)	204.43 (0.48)	243.81 (7.16)
0.9797	One endotherm						190.95 (1.18)	201.41 (0.02)	202.09 (0.07)	204.23 (0.11)	246.09 (5.68)
0.9905	One endotherm						182.37 (1.71)	201.24 (0.07)	202.05 (0.12)	203.98 (0.32)	247.55 (5.92)
1.000	One endotherm						194.51 (0.69)	201.40 (0.03)	202.11 (0.13)	204.22 (0.44)	248.94 (3.77)

1 Mid-point between endotherms is used as an approximation of the baseline offset temperature of the low-temperature endotherm. This separation also provides the calculation of the enthalpy of both the low- and high-temperature endotherms, when possible.

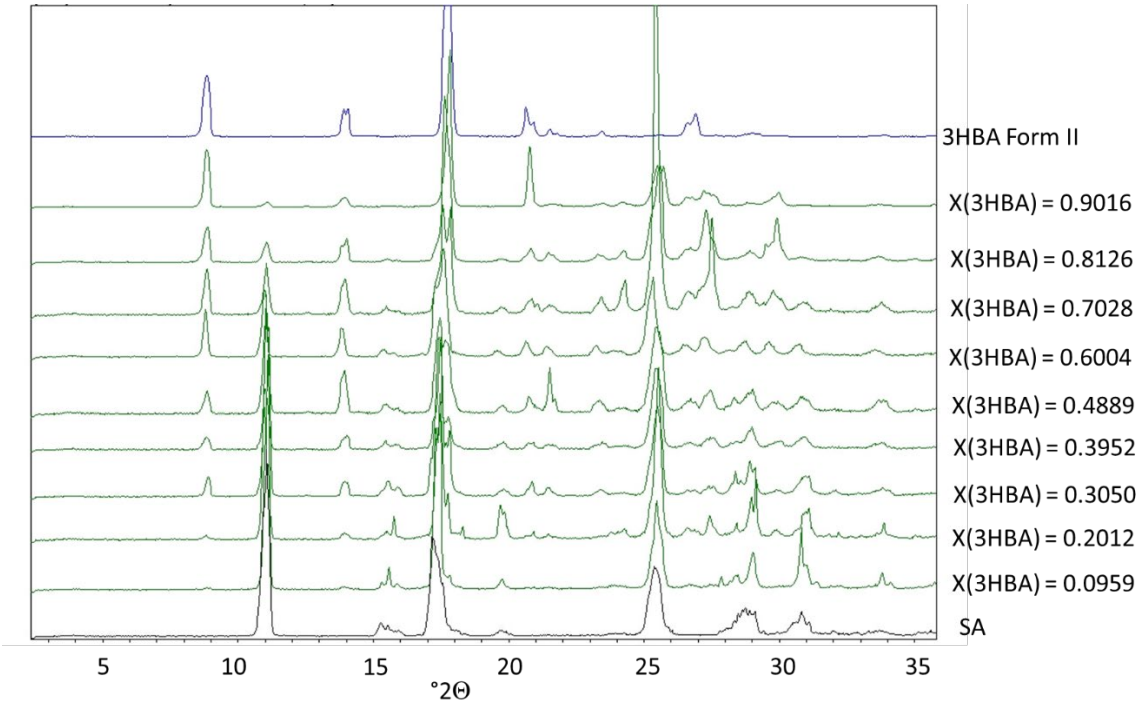

Figure 2. XRPD overlay of select SA-3HBA Form II samples used in DSC analyses prepared via evaporative crystallization from MeOH.

Table 2. DSC summary for SA-3HBA Form II

X(3HBA)	DSC endotherms	Low temperature endotherm					High temperature endotherm				
mol 3HBA/mol SA+3HBA		T_{inset}	T_{onset}	T_{peak}	T_{offset}	Enthalpy	T_{inset}	T_{onset}	T_{peak}	T_{offset}	Enthalpy
		°C	°C	°C	°C	J/g	°C	°C	°C	°C	J/g
0	One endotherm						154.07 (0.08)	158.64 (0.006)	159.16 (0.09)	160.98 (0.23)	189.56 (4.21)
0.0038	One endotherm						152.60 (0.73)	158.06 (0.12)	159.13 (0.09)	161.09 (0.15)	185.24 (5.02)
0.0062	One endotherm						154.04 (0.51)	158.01 (0.22)	158.85 (0.12)	160.85 (0.20)	184.04 (6.26)
0.0079	One endotherm						152.59 (0.28)	157.74 (0.11)	158.81 (0.16)	160.93 (0.24)	180.93 (1.96)
0.0103	Two separated endotherms	141.72 (0.41)	142.71 (0.08)	144.12 (0.06)	145.88 (0.39)	1.50 (0.38)	149.41 (0.36)	157.27 (0.34)	158.89 (0.09)	160.63 (0.22)	171.06 (9.7)
0.0307	Two partially overlapping endotherms	140.28 (0.24)	143.50 (0.12)	144.63 (0.02)	146.50[1] (0.28)	13.56 (0.47)		154.31 (0.06)	157.66 (0.14)	159.72 (0.25)	162.64 (5.19)
0.0508	Two partially overlapping endotherms	139.11 (0.11)	143.41 (0.10)	144.76 (0.01)	146.54[1] (0.24)	31.30 (2.31)		152.63 (0.25)	156.53 (0.18)	158.67 (0.23)	146.43 (2.99)
0.0699	Two partially overlapping endotherms	138.45 (0.42)	143.52 (0.04)	144.80 (0.03)	146.88[1] (0.07)	49.12 (6.83)		150.92 (1.45)	155.47 (0.38)	158.18 (0.24)	129.74 (2.87)
0.0959	Two partially overlapping endotherms	138.66 (0.53)	142.18 (0.02)	144.78 (0.08)	147.14[1] (0.07)	67.36 (2.24)		150.87 (2.16)	154.66 (0.31)	157.27 (0.62)	112.64 (5.16)
0.2012	Two endotherms mostly overlapping	137.48 (0.56)	142.22 (0.02)	144.59 (0.04)		152.40 (0.45)				152.64 (1.22)	35.88 (3.40)
0.2489	Two endotherms mostly overlapping	138.18 (0.19)	142.19 (0.02)	144.05 (0.23)		173.28 (2.16)				151.98 (1.64)	17.22 (0.35)
0.3050	Two endotherms mostly overlapping	137.90 (0.30)	142.44 (0.20)	143.92 (0.17)		178.83 (5.37)	Not accessible due to form transformation				
0.3952	Two endotherms mostly overlapping	137.48 (0.95)	142.30 (0.03)	143.80 (0.20)		170.72 (3.37)	Not accessible due to form transformation				
0.4889	Two partially overlapping endotherms and one exotherm	138.83 (1.03)	142.24 (0.04)	144.12 (0.20)	146.53[1] (0.28)	140.28 (6.02)	Not accessible due to form transformation				

0.6004	Two partially overlapping endotherms and one exotherm	138.77 (0.18)	142.04 (0.04)	143.77 (0.15)	145.98 (0.29)	103.71 (2.69)	Not accessible due to form transformation
0.7028	Two partially overlapping endotherms and one exotherm	138.47 (0.25)	141.98 (0.09)	143.38 (0.09)	145.62 (0.34)	69.12 (4.32)	Not accessible due to form transformation
0.8126	Two partially overlapping endotherms and one exotherm	137.30 (0.13)	141.65 (0.04)	143.18 (0.12)	145.19 (0.27)	49.83 (3.75)	Not accessible due to form transformation
0.9016	Two mostly separated endotherms and one exotherm	136.04 (0.95)	140.86 (0.12)	142.60 (0.11)	144.42 (0.37)	18.83 (2.80)	Not accessible due to form transformation
0.9513	Two separated endotherms and one exotherm	134.94 (1.13)	139.76 (0.10)	141.99 (0.08)	144.11 (0.49)	8.1 (0.78)	Not accessible due to form transformation
0.9754	Two separated endotherms and one exotherm	134.07 (0.97)	135.95 (2.34)	139.61 (1.45)	142.81 (0.24)	3.30 (0.23)	Not accessible due to form transformation
0.9904	One endotherm						Not accessible due to form transformation
1.000	One endotherm						Not accessible due to form transformation

1 Mid-point between endotherms is used as an approximation of the baseline offset temperature of the low-temperature endotherm. This separation also provides the calculation of the enthalpy of both the low- and high-temperature endotherms, when possible.

Table 3. DSC summary for SA-3HBA Form II: Exothermic transition from Form II (or βII) to Form I (or βI) of 3HBA

X(3HBA)	T_{inset}	T_{onset}	T_{peak}	T_{offset}	Enthalpy of exotherm
mol 3HBA/mol SA+3HBA	°C	°C	°C	°C	J/g
0.4889	156.64 (1.39)	158.50 (0.93)	161.60 (0.77)	165.33 (0.71)	15.1 (1.12)
0.6004	154.37 (0.17)	156.09 (0.18)	158.94 (0.17)	161.6 (0.27)	7.69 (0.72)
0.7028	154.76 (2.82)	160.73 (0.25)	164.02 (0.27)	168.71 (2.09)	11.32 (1.07)
0.8126	153.27 (0.63)	158.05 (0.31)	162.39 (0.19)	167.10 (0.37)	10.26 (1.11)
0.9016	158.33 (1.47)	160.50 (0.93)	164.98 (0.95)	170.32 (0.37)	6.21 (2.62)
0.9513	161.18 (1.39)	163.11 (2.05)	167.76 (2.19)	171.99 (1.78)	2.47 (0.19)
0.9754	154.59 (3.02)	156.23 (3.62)	160.43 (2.57)	165.55 (2.43)	2.43 (0.92)
0.9904	145.73 (2.00)	147.64 (2.01)	152.78 (0.98)	159.36 (0.77)	1.83 (0.38)
1.000	142.21 (2.20)	143.41 (1.57)	150.40 (0.74)	159.36 (2.31)	3.17 (0.31)

Table 4. Solid-Liquid Equilibria (SLE) summary of SA-3HBA Form I in 40 w% MeOH in H2O at 25°C

Solid phase	Liquid	Solid	Conc. of SA	Conc. of 3HBA	X(SA)	X(3HBA)	X(solvent)
	w% or mol% 3HBA in SA	w% or mol% 3HBA in SA	mg SA/g solvent	mg 3HBA/g solvent	mmol SA/(mol total)	mmol 3HBA/(mol total)	mol solvent/(mol total)
SA	0.00%	0.00%	23.37	0.00	3.6813	0.0000	0.9963
α	18.25%	0.04%	26.81	5.99	4.2173	0.9416	0.9948
α	26.67%	0.08%	27.63	10.04	4.3423	1.5788	0.9941

α	37.37%	0.09%	29.52	17.61	4.6327	2.7639	0.9926
α	40.57%	0.13%	29.78	20.33	4.6723	3.1897	0.9921
α	55.26%	0.26%	34.06	42.06	5.3211	6.5720	0.9881
α	60.84%	0.39%	39.53	61.41	6.1523	9.5570	0.9843
α	65.38%	0.45%	43.14	81.46	6.6895	12.6310	0.9807
α+βI	69.47%	0.65%	51.83	117.96	7.9809	18.1642	0.9739
α+βI	70.27%	48.72%	52.21	123.39	8.0317	18.9833	0.9730
α+βI	69.64%	78.71%	53.47	122.65	8.2254	18.8676	0.9729
α+βI	70.35%	91.47%	52.15	123.72	8.0221	19.0337	0.9729
βI	79.26%	99.58%	29.48	112.63	4.5586	17.4181	0.9780
βI	77.79%	99.59%	32.93	115.38	5.0883	17.8253	0.9771
βI	85.36%	99.70%	18.60	108.40	2.8825	16.8022	0.9803
βI	87.84%	99.79%	14.53	104.99	2.2547	16.2929	0.9815
βI	85.06%	99.80%	19.31	109.87	2.9914	17.0254	0.9800
βI	94.51%	99.85%	6.17	106.17	0.9581	16.4948	0.9825
βI	96.94%	99.93%	3.16	100.18	0.4924	15.5864	0.9839
3HBA, Form I	100%	100%	0.00	98.36	0.0000	15.3148	0.9847

Table 5. Solid-Liquid Equilibria (SLE) summary of SA-3HBA Form II in 40 w% MeOH in H2O at 25°C

Solid phase	Liquid	Solid	Conc. of SA	Conc. of 3HBA	X(SA)	X(3HBA)	X(solvent)
	w% or mol% 3HBA in SA	w% or mol% 3HBA in SA	mg SA/g solvent	mg 3HBA/g solvent	mmol SA/(mol total)	mmol 3HBA/(mol total)	mol solvent/(mol total)
SA	0.00%	0.00%	23.37	0.00	3.6813	0.0000	0.9963
α	18.25%	0.04%	26.81	5.99	4.2173	0.9416	0.9948
α	26.67%	0.08%	27.63	10.04	4.3423	1.5788	0.9941
α	37.37%	0.09%	29.52	17.61	4.6327	2.7639	0.9926
α	40.57%	0.13%	29.78	20.33	4.6723	3.1897	0.9921
α	55.26%	0.26%	34.06	42.06	5.3211	6.5720	0.9881
α	60.84%	0.39%	39.53	61.41	6.1523	9.5570	0.9843
α	65.38%	0.45%	43.14	81.46	6.6895	12.6310	0.9807
α+βII	73.37%	9.21%	60.17	165.79	9.1853	25.3108	0.9655
α+βII	72.92%	40.33%	60.31	162.41	9.2120	24.8068	0.9660
α+βII	72.58%	58.11%	62.02	164.14	9.4682	25.0573	0.9655
βII	80.93%	99.68%	35.59	150.99	5.4658	23.1907	0.9713
βII	86.61%	99.73%	22.53	145.77	3.4707	22.4509	0.9741
βII	87.77%	99.81%	19.89	142.76	3.0654	22.0069	0.9749
βII	93.04%	99.82%	10.32	137.85	1.5943	21.2985	0.9771
3HBA, Form II	100.00%	100.00%	0.00	130.54	0.0000	20.2229	0.9798

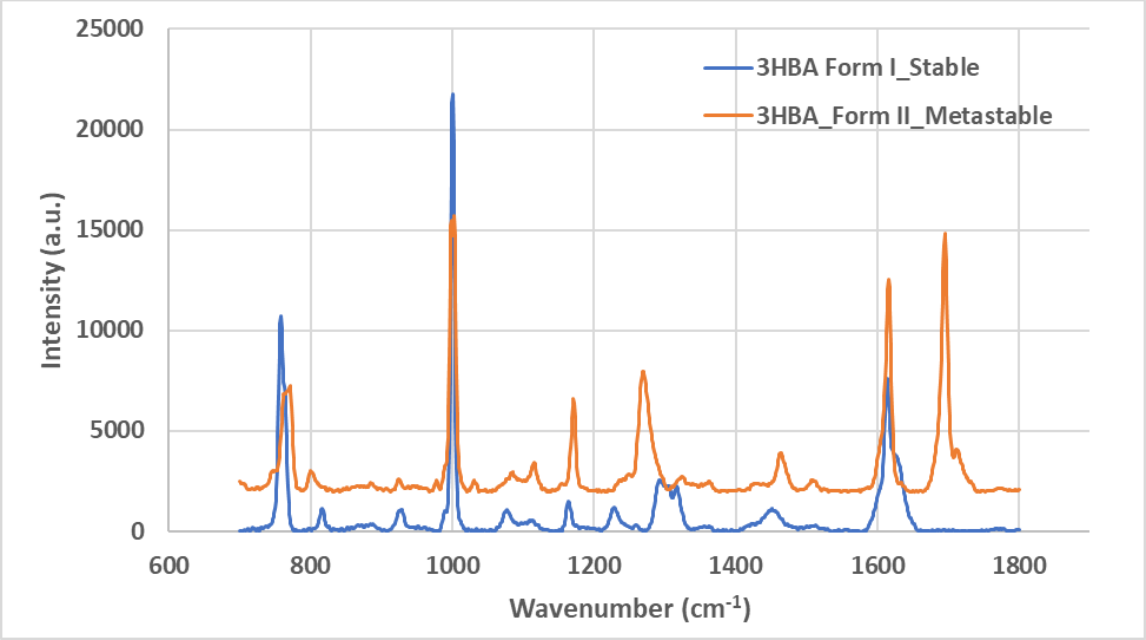

Figure 3. Reference spectra for 3HBA Form I and II. Peak area between 1685 and 1705 cm^{-1} were used as reference to monitor polymorphic conversion rate

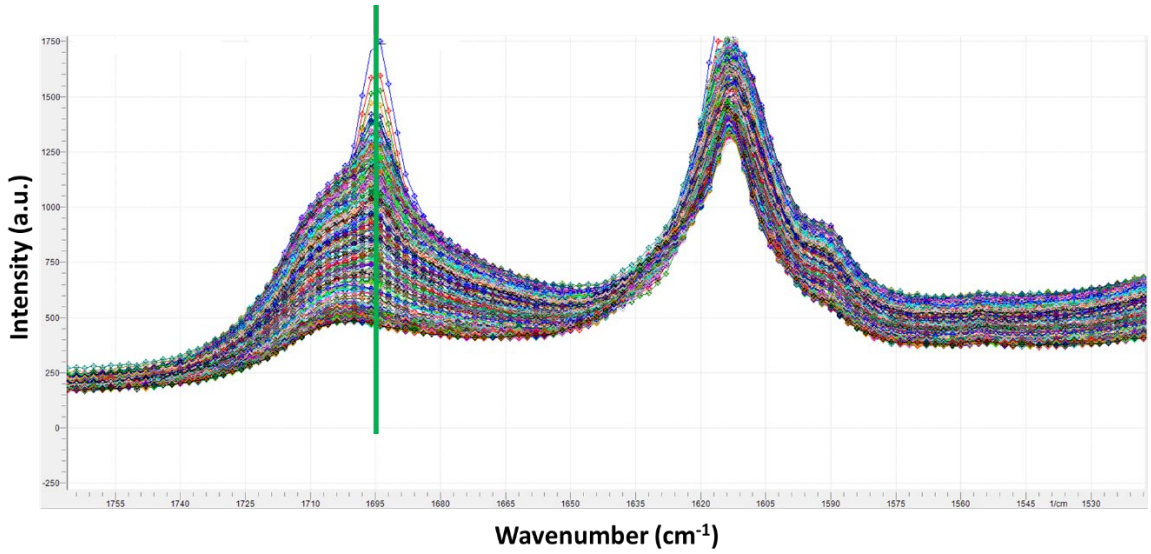

Figure 4. Example of changes in Raman spectra during a form conversion (wavelength: 1800 – 1500 cm^{-1})

Thermodynamic Modelling via NRTL

Fitting the Liquid BIPs $\Delta g_{12}^{L,\pi}$ and $\Delta g_{21}^{L,\pi}$

As mentioned in the text, for the liquid-state NRTL BIPs of 3-hydroxybenzoic acid (1) and salicylic acid (2), Δg_{12}^{L} and Δg_{21}^{L} were not expressed as functions of temperature due to the sparsity of solid-liquid equilibrium melt data (i.e., the SSLE data at the eutectic temperature). As also explained in the text, the Δg_{12}^{L} and Δg_{21}^{L} were treated separately for the equilibria involving βI and βII. Hence, we can succinctly denote the two different parameter sets as $\left\{\Delta g_{12}^{L,\pi}, \Delta g_{21}^{L,\pi}\right\}$, where π denotes the β-phase (I or II) involved in the phase equilibria.

As performed in our earlier study [Wang, Y. Ricci, F., Nordstrom, F.L., Terminal crystalline solid solutions and T-X phase diagram of salicylic acid – 4-hydroxybenzoic acid, Phys. Chem. Chem. Phys, 2024, 26, 3069.], a more in-depth study $\Delta g_{12}^{L,\pi}$ and $\Delta g_{21}^{L,\pi}$ was performed to assess the degeneracy of the liquid parameters with respect to the SSLE criteria which must be satisfied simultaneously:

$$\left\{\gamma_i^{\alpha} x_i^{\alpha} f_i^{S}/f_i^{L} = \gamma_i^{L} x_i^{L} = \gamma_i^{\beta\pi} x_i^{\beta\pi} f_i^{S}/f_i^{L}\right\}_{i=1,2} \tag{S1}$$

Numerically, the regression procedure requires determination of the parameters $\Delta g_{12}^{L,\pi}$ and $\Delta g_{21}^{L,\pi}$ to calculate γ_i^{L} (provided known values of Δg_{12}^{S} and Δg_{21}^{S}, which we obtained from regressing the solvus data to the T-dependent expressions described in the text, and hence known values of γ_i^{S}). This was done by driving the objective function shown below to zero:

$$OF = \sum_{i=1}^{2}\left(\gamma_i^{\alpha} x_i^{\alpha} f_i^{S}/f_i^{L} - \gamma_i^{L} x_i^{L}\right)^2 + \left(\gamma_i^{\beta\pi} x_i^{\beta\pi} f_i^{S}/f_i^{L} - \gamma_i^{L} x_i^{L}\right)^2 \tag{S2}$$

Because there are only two regression parameters in the above equation ($\Delta g_{12}^{L,\pi}$ and $\Delta g_{21}^{L,\pi}$), one can easily visualize how the OF varies with the parameter values. Contour plots showing this functional dependency for both the βI and βII systems are illustrated below. These contour plots were used to locate the approximate minimum of the OF, and the corresponding approximate values of $\Delta g_{12}^{L,\pi}$ and $\Delta g_{21}^{L,\pi}$ were used as initial guesses in the regression algorithm.

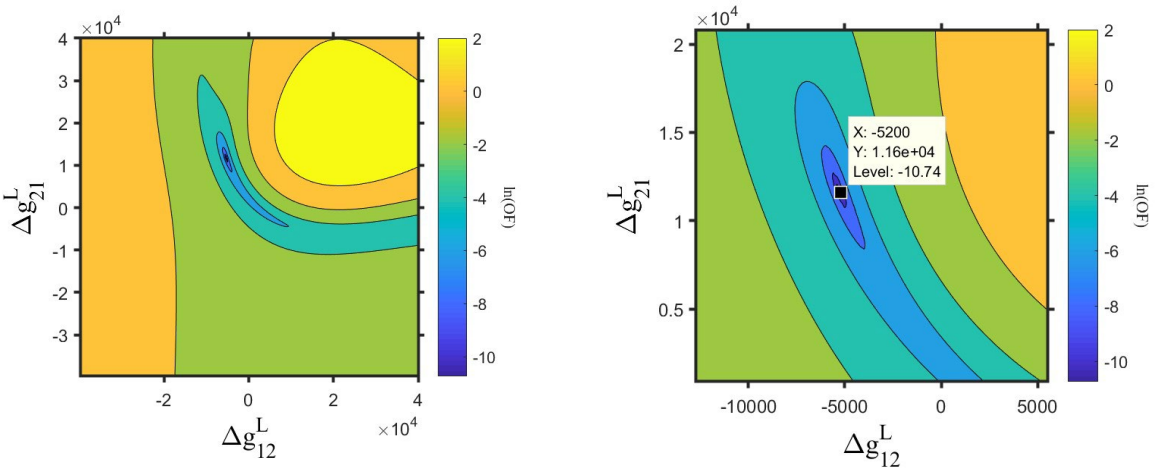

Figure 5. Objective function at SSLE (α-βI-L), with varying values of $\Delta g_{12}^{L,I}$ and $\Delta g_{21}^{L,I}$. The right pane shows a zoomed view, with the data cursor showing the approximate location of the minimum.

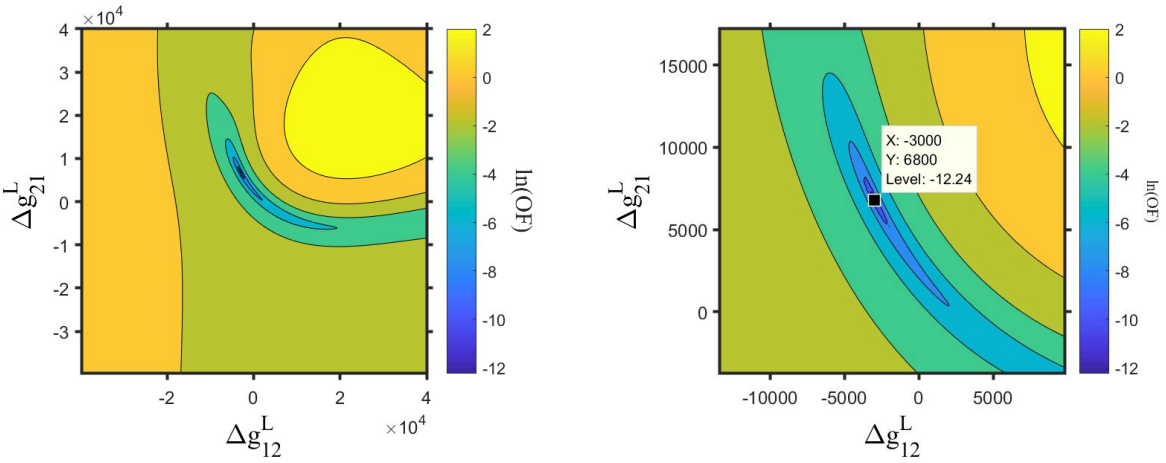

Figure 6. Objective function at SSLE (α-βII-L), with varying values of $\Delta g_{12}^{L,II}$ and $\Delta g_{21}^{L,II}$. The right pane shows a zoomed view, with the data cursor showing the approximate location of the minimum.

We also note that it was attempted to predict the α-βII T-X phase diagram using the Δg_{12}^{L} and Δg_{21}^{L}values regressed to the α-βI data (e.g., $\{\Delta g_{12}^{L,I}, \Delta g_{21}^{L,I}\}$); however, the predicted eutectic composition was in significant error. A potentially more accurate approach for using only one set of $\{\Delta g_{12}^{L}, \Delta g_{21}^{L}\}$ would be to regress these two parameters to both the α-βI and α-βII phase equilibria simultaneously.

NRTL Parameter Values

The regressed NRTL BIP values are provided below. We note once again that the non-randomness parameters (α_{ij}) were all taken as 0.2 for both the solid and liquid state models. We reiterate that the liquid state BIPS for components 1 and 2 $\{\Delta g_{12}^{L,I}, \Delta g_{21}^{L,I}\}$ and $\{\Delta g_{12}^{L,II}, \Delta g_{21}^{L,II}\}$ were regressed to SSLE data in the 1-2 system (i.e., with respect to the two solid solutions in equilibrium with the eutectic melt). The other liquid state BIPs involving the solvent (e.g., $\Delta g_{13}^{L,I}$, etc…) were regressed to the solubility data in 40 w% MeOH in H_2O, where this fixed-composition binary solvent mixture was treated as a pseudo pure solvent.

Table 6. NRTL Solid State BIPs

$\Delta g_{12}^{S,I}$:	
	$c_{12}^{S,I}$ = 18185.8959 J/mol
	$d_{12}^{S,I}$ = -32.149 J/mol-K
$\Delta g_{21}^{S,I}$:	
	$c_{21}^{S,I}$ = -3747.1294 J/mol
	$d_{21}^{S,I}$ = 41.4138 J/mol-K
$\Delta g_{12}^{S,II}$:	
	$c_{12}^{S,II}$ = 11139.8254 J/mol
	$d_{12}^{S,II}$ = -6.839 J/mol-K
$\Delta g_{21}^{S,II}$:	
	$c_{21}^{S,II}$ = -453.2698 J/mol
	$d_{21}^{S,II}$ = 28.9163 J/mol-K

Table 7. NRTL Liquid State BIPs

$\Delta g_{12}^{L,I}$	-5230.7972 J/mol
$\Delta g_{21}^{L,I}$	11619.6266 J/mol
$\Delta g_{13}^{L,I}$	19762.0553 J/mol
$\Delta g_{31}^{L,I}$	-6585.69442 J/mol
$\Delta g_{23}^{L,I}$	-4161.09328 J/mol
$\Delta g_{32}^{L,I}$	11119.0683 J/mol
$\Delta g_{12}^{L,II}$	-3002.0537 J/mol
$\Delta g_{21}^{L,II}$	6858.9432 J/mol
$\Delta g_{13}^{L,II}$	-9017.86118 J/mol
$\Delta g_{31}^{L,II}$	17803.6867 J/mol
$\Delta g_{23}^{L,II}$	-7094.86151 J/mol
$\Delta g_{32}^{L,II}$	18299.0624 J/mol